

# Autodetachment of diatomic carbon anions from long-lived high-rotation quartet states

Viviane C. Schmidt

*Max-Planck-Institut für Kernphysik, Saupfercheckweg 1, 69117 Heidelberg, Germany*

Roman Čurík\*

*J. Heyrovský Institute of Physical Chemistry, ASCR, Dolejškova 3, 18223 Prague, Czech Republic*

Milan Ončák

*Institut für Ionenphysik und Angewandte Physik,  
Leopold-Franzens-Universität Innsbruck, Technikerstraße 25/3, Innsbruck 6020, Austria*

Klaus Blaum, Sebastian George, Jürgen Göck, Manfred Grieser, Florian Grussie, Robert von Hahn,<sup>†</sup>

Claude Krantz, Holger Kreckel, Oldřich Novotný, Kaija Spruck, and Andreas Wolf

*Max-Planck-Institut für Kernphysik, Saupfercheckweg 1, 69117 Heidelberg, Germany*

(Dated: September 18, 2024)

We show that strong molecular rotation drastically modifies the autodetachment of  $C_2^-$  ions in the lowest quartet electronic state  $a^4\Sigma_u^+$ . In the strong-rotation regime, levels of this state only decay by a process termed “rotationally assisted” autodetachment, whose theoretical description is worked out based on the non-local resonance model. For autodetachment linked with the exchange of six rotational quanta, the results reproduce a prominent, hitherto unexplained electron emission signal with a mean decay time near 3 milliseconds, observed on stored  $C_2^-$  ions from a hot ion source.

Properties and decay mechanisms of highly excited small molecules attract wide interest in fields such as molecular astrophysics [1, 2], atmospheric science [3], optical control of chemical reactions [4] and plasma processing [5]. Thus, recently, extreme rotational excitation created by optical excitation was found to enhance the reactivity of trapped diatomic cations [4], while signatures of strongly rotating diatomic radicals were even found in astrophysical observations [2, 6]. Diatomic anions with similarly high excitation are being studied using stored ion beams [7–9]. Here, highly excited molecules are created by fast-ion sputtering from solid surfaces [10, 11], where they acquire rotational and vibrational energy up to the dissociation limit [12]. Studies at ion storage rings [13–16] revealed the stability properties of such anionic molecules when emitting either the excess electron (autodetachment) or a heavy constituent (autofragmentation). Recently observed autodetachment on these systems [15] was attributed to high vibrational excitation [15, 17].

The present work focuses on decay processes at high internal excitation for stored diatomic carbon anions  $C_2^-$ . Unique among the small molecular anions,  $C_2^-$  has low-lying electronic states sharing with the ground state the doublet spin symmetry and enabling optical spectroscopy [18] and even laser cooling [19]. Correspondingly, most of its higher vibrational levels decay by electronic radiative transitions, while rotational excitation is much more stable, a permanent dipole moment still being absent in the homonuclear system. Hence, by storing the  $C_2^-$  anions extracted from a hot source, properties of this molecule

can be investigated at high, mainly rotational excitation.

In this Letter, we analyze the autodetachment of  $C_2^-$  under such excitation conditions. Based on previous observations [20–23] autodetachment of  $C_2^-$  from a hot ion source leads to a prominent near-exponential decay signal with a time constant close to 3 ms, which could not be linked to rates of any competing radiative decay [21, 22]. No conclusive explanation could so far be given for the process behind these observations.

We show that this temporal behavior likely indicates a drastic modification of autodetachment in the lowest quartet state of  $C_2^-$  by strong molecular rotation. At low rotation, the electronic energy of this state lies  $\sim 4$  eV above the anionic doublet ground state and  $\sim 1.4$  eV above the detachment energy to neutral  $C_2$ . Direct diabatic autodetachment (AD) then leads to pico- to femtosecond lifetimes of any quartet levels. However, rotation up-shifts the relevant minima of the electronic potentials more strongly for the neutral than for the anionic quartet states. At sufficient rotation, quartet levels appear for which AD is energetically forbidden *at fixed rotation* and can only proceed when the rotational state changes during the AD process. We develop the theoretical description of such processes, which we term “rotationally assisted” AD. Our calculated rates show that AD from rotationally excited  $C_2^-$  ions in the lowest quartet state, connected with a change of internal rotation by six quanta, well explains the observed AD signal. The results also show that this AD signal represents a limited range of rotational excitation and that more stable quartet  $C_2^-$  ions should exist at even stronger rotation.

The AD of vibrationally excited levels in the  $A^2\Pi_u$  and  $B^2\Sigma_u^+$  states of  $C_2^-$  was observed by electron spectroscopy [24, 25] using laser excitation from the  $X^2\Sigma_g^+$  ground state. The required excitation energy is given by the  $C_2^-$  detachment threshold (3.269 eV [26]). Resonances in the electron energy spectra were mainly assigned to AD from levels in the  $B^2\Sigma_u^+$  state (vibrational quantum number  $v \geq 5$ ) and indicate AD lifetimes of  $\lesssim 10^{-8}$  s. In fact, considering also radiative decay [27], all  $B^2\Sigma_u^+$  levels are expected to live for  $< 0.1 \mu\text{s}$ . For AD from levels in the  $X^2\Sigma_g^+$  and  $A^2\Pi_u$  states of  $C_2^-$ , high vibrational excitation ( $v \geq 16$  [26]) is necessary and the processes were hardly observable so far. As a source of the prominent 3 ms AD signal observed on excited  $C_2^-$ , these levels are unlikely as their population would require extremely high vibrational temperature in view of the high detachment threshold. The theoretically predicted [28–32] lowest quartet state of  $C_2^-$ ,  $a^4\Sigma_u^+$ , thus logically enters as a further possible source of the stored-beam  $C_2^-$  AD signal. This was already speculatively considered [21, 22]. However, to our best knowledge, no further specification about the role of this state in the AD of excited  $C_2^-$  was given previously. Moreover, we are not aware of any experimental spectroscopic characterization of the quartet state in free  $C_2^-$ .

Our theoretical study is partly based on earlier investigations on the stability of rotating anions [33–35]. Similar to the methods of that work, our approach explicitly allows for electronically unstable initial anion states of resonant character, using a diabatic representation and employing the non-local resonance model [36, 37]. This method fundamentally differs from that appropriate for the AD rates from doublet  $C_2^-$  [24], based on non-adiabatic perturbation of adiabatic molecular levels as introduced by Berry [38].

In a companion paper (CP) [39] we present experimental results on electron emission (AD) as well as heavy-particle autofragmentation (AF) using  $C_2^-$  ions from a hot ion source injected into a cryogenic ion storage ring. Moreover, we develop a detailed model of  $C_2^-$  at high rotational and vibrational excitation that includes the radiative decay as well as the AD and AF rates for all relevant levels in the  $X^2\Sigma_g^+$ ,  $A^2\Pi_u$  and  $a^4\Sigma_u^+$  states. Together with a model of the level populations, these data complement the rates of rotationally assisted AD calculated here and allow us to show that AD and AF from  $a^4\Sigma_u^+$   $C_2^-$  ions can plausibly explain the observed signals of both types in their intensities and their temporal behaviour. Below, we shortly summarize the experimental AD signal and then present our theoretical method to assess the stability and the rotationally assisted AD decay of quartet  $C_2^-$ .

The detected AD and AF count rates from a stored  $C_2^-$  beam following its injection into a storage ring are shown in Fig. 1. These data were obtained at the cryogenic storage ring CSR at the Max Planck Institute for

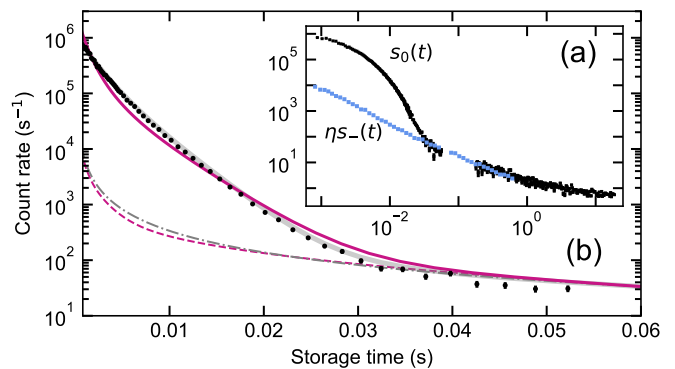


FIG. 1. Count rates by electron emission (AD) and dissociation (AF) from  $C_2^-$  as functions of the storage time  $t$  [39]. (a) Signals  $s_0$  and  $\eta s_-$  (see the text) with  $\eta = 0.75$ . (b) Neutral signal  $s_0$ , assigned to AD and AF, with data shown as symbols. Thick grey line: fit using a bi-exponential time dependence ( $\tau_{1,2}$ ) of the AD signal and including a background (dashed, grey) from AF varying as  $\propto t^c$  with  $c = -1.287$ , resulting from a fit to  $\eta s_-$  at  $t < 0.06$  s in (a). Purple lines: sum  $s_d + \eta s_f$  of modeled AD and AF from  $C_2^-$  in the  $a^4\Sigma_u^+$  state (solid) and modeled AF background  $\eta s_f$  (dashed-dotted).

Nuclear Physics in Heidelberg, Germany, as described in the CP [39]. The ions are produced in a sputter ion source and accelerated to 60 keV. About  $4 \times 10^7$  ions are then injected into the ring and stored. Products of unimolecular decay are separated from the stored beam at the deflectors of the storage ring by their differing charge-to-mass ratios. In separate runs, a single counting detector behind one of the deflectors was placed to intersect either neutral fragments ( $C_2$  or  $C$ , count rate  $s_0$ ) or  $C^-$  fragments ( $s_-$ ). Products following electron emission (AD) contribute to  $s_0$  only, while each dissociation event (AF) contributes to  $s_0$  and  $s_-$ . The cryogenic cooling of the storage ring leads to extreme vacuum such that  $C_2^-$  destruction in collisions with residual gas molecules occurs too rarely to contribute significantly to the count rates. Also, overall ion beam loss is expected to be insignificant during the displayed storage time interval.

The rate  $s_0$  of neutrals shows a strong initial peak not appearing in  $s_-$ , thus corresponding to the AD signature. The temporal dependence of this AD component is close to exponential, consistent with the time constant near 3 ms observed earlier [21, 22]. We extract the AD component as  $s_0 - \eta s_-$  with a near-unity factor  $\eta$  compensating intensity fluctuations between the runs [39]. This component is well fitted by a bi-exponential decay with time constants  $\tau_1 = 3.31(4)$  ms and  $\tau_2 = 1.56(5)$  ms.

The complete picture of coexistent decay by AD, AF, and radiative relaxation is discussed in the CP [39]. It turns out that for levels showing AD, decay by AF is mostly negligible. Moreover, radiative decay can significantly compete with AF, but is typically insignificant with respect to AD. The decay constants of the exper-

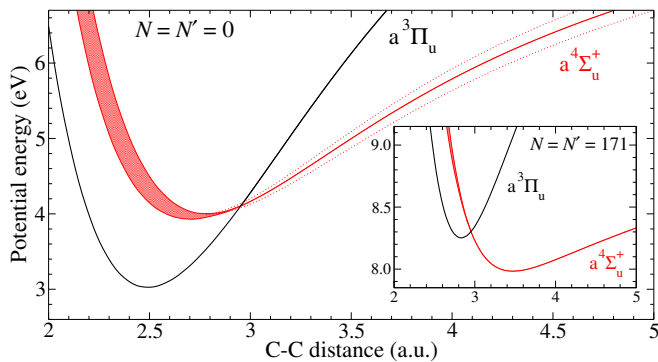


FIG. 2. Potential curves of (red)  $C_2^-(a^4\Sigma_u^+)$  and (black)  $C_2(a^3\Pi_u)$  referred to the  $C_2^-$  rovibrational ground state, neglecting nuclear rotation. Red-shaded:  $R$ -dependent width of the  $a^4\Sigma_u^+$  AD resonance; dotted: *ab initio* uncertainty of the bound-state potential. Inset: Potential curves including the centrifugal term of Eq. (2) setting  $N = 171$  for the anion and  $N' = N$  for the neutral.

imental AD component,  $\tau_{1,2}$ , therefore reflect observed lifetimes against AD.

Neglecting nuclear rotation, the  $C_2^-(a^4\Sigma_u^+)$  state can decay by spin-allowed AD into  $C_2(a^3\Pi_u)$ . While predicted in multiple theoretical studies [28–32, 40] this quartet anionic state could never be unambiguously assigned to any feature measured on free  $C_2^-$  [21, 22, 41, 42]. For the present work, *ab initio* calculations were performed [39] using the MOLPRO package [43] to consistently locate this and the three lower lying anionic states together with the first two neutral states of  $C_2$ . Rotationless potential energy curves of the anionic  $a^4\Sigma_u^+$  and neutral  $a^3\Pi_u$  states are shown as a function of the internuclear distance  $R$  in Fig. 2. For some  $R$  range,  $C_2^-(a^4\Sigma_u^+)$  lies above  $C_2(a^3\Pi_u)$  and forms an electronic resonance. The resonance width at the molecular equilibrium position in the absence of nuclear rotation amounts to 0.48 eV [40] and in this case enables very fast AD with pico- to femtosecond lifetimes. In the bound-state part ( $R > 3$  a.u.) we complemented the available resonance calculations [40, 44] by our  $a^4\Sigma_u^+$  *ab initio* results whose uncertainty reaches  $\pm 170$  meV at  $R = 5$  a.u. [45] (see Fig. 2).

The arrangement of the curves changes for high rotations because of the significant centrifugal potential. For a  $C_2^-$  nuclear rotation quantum number  $N \geq 155$  [39] and assuming the quantum number  $N'$  of the neutral molecule to be  $N' = N$ , the  $v = 0$  level of the anionic  $a^4\Sigma_u^+$  curve lies below that of the neutral  $a^3\Pi_u$  curve. This form of a rearrangement of the neutral and anionic curves for higher rotational states was previously documented for  $N = 20$ –40 of the  $H_2^-$  and  $D_2^-$  ions [33, 35, 56]. The present, heavier molecule with a smaller rotational constant requires much higher  $N$  for a similar rearrangement. Considering, e.g.,  $N = N' = 171$  (Fig. 2), the  $a^4\Sigma_u^+$  ( $v = 0$ ) energy clearly lies below all  $v$ -

levels of the neutral triplet state. Quartet levels up to a certain  $v$  then cannot undergo AD. However, such rotationally stabilized levels are in fact not absolutely stable against AD, since processes with  $N' < N$  for high enough  $|N' - N|$  become energetically allowed again. This calls for the AD rate calculations to include such changes of the nuclear rotation.

A theory describing rotationally assisted AD of  $C_2^-$  requires combining two approaches. The first one was used to predict the rotationally stabilized anion states of  $H_2^-$  and its isotopologues [33, 35]. However, this technique did not allow for a change of the electronic angular momentum  $l$  and kept it fixed in the  $p$  wave. When applied to the present case, such limited rotational change of the molecular frame during the AD process predicts lifetimes  $< 10^{-10}$  s for the  $a^4\Sigma_u^+$  levels. A here incorporated second step corrects these shortcomings by accounting for the rotational degrees of freedom within the non-local resonance model [36]. Its derivation for  $\Sigma$ -states of anion and neutral can be found in Ref. [57]. A similar procedure, based on the local complex potential was developed for the description of the angular distributions of the molecular fragments resulting from the dissociative electron attachment process [58].

Along this line, we extend the non-local resonance model underlying the work by Čížek *et al.* [33–35, 57]. For the non-dissociative states  $|\Phi\rangle$  and the narrow resonances, the diagonalization of the effective complex Hamiltonian  $H^{\text{eff}}$  provides the resonance energy  $E$  as

$$H^{\text{eff}}(E)|\Phi\rangle = E|\Phi\rangle. \quad (1)$$

The energy dependence of  $H^{\text{eff}}$  leads to an iterative procedure that usually converged within a few iterations in the present study. The effective nuclear Hamiltonian  $H^{\text{eff}}$  plays a central role in projection-operator methods that have been previously used to study AD [33, 34], dissociative electron attachment [58–61], vibrational excitation [62–64], and associative detachment [65, 66]. In its local form it can be written, for each of the initial anion's rotational states  $N$ , as [45]

$$H_N^{\text{eff}} = T + \frac{N(N+1)}{2\mu R^2} + V_r(R) - \frac{i}{2}\Gamma_N(R). \quad (2)$$

Here  $T$  is the radial nuclear kinetic energy operator and  $V_r(R)$  the real part of the anion's potential. Moreover,

$$\Gamma_N(R) = \sum_{lN'\nu'\eta'} g_{lN'\nu'}^{\eta'} (2N'+1) \begin{pmatrix} l & N' & N \\ \Lambda & -\Lambda & 0 \end{pmatrix}^2 \times \Gamma_l(R) |\chi_{\nu'N'}(R)|^2, \quad (3)$$

is the  $R$ -dependent total width, where  $\Gamma_l(R)$  is the local partial width for partial wave  $l$ ,  $\chi_{\nu'N'}(R)$  describes the final rovibrational states of the neutral molecule, and the factor  $g_{lN'\nu'}^{\eta'} = 0$  or 1 selects only one of the two final,

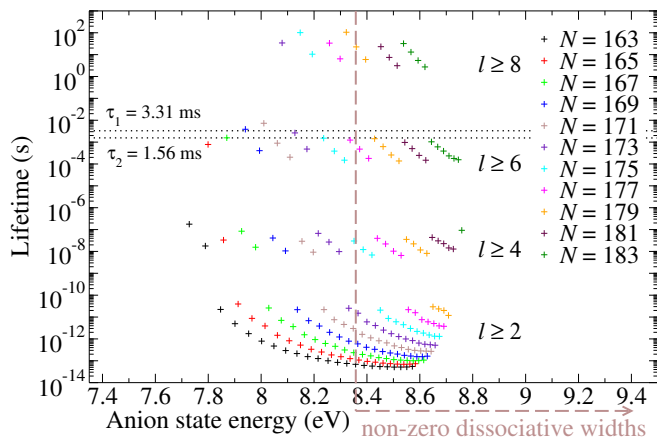


FIG. 3. Energies and lifetimes  $\tau_{AD}$  of anion states  $v, N$ , color-coded according to  $N$ , with the partial wave ( $l$ ) range of separated groups, the threshold for tunneling predissociation (long-dashed line), and the experimental time constants  $\tau_{1,2}$ .

nearly degenerate  $a^3\Pi_u$  states (hence,  $\Lambda = 1$ ) in order to preserve the nuclear spin state during the AD process [45]. The imaginary part, Eq. (3), of  $H^{\text{eff}}$ , Eq. (2), clearly shows how the lifetime of the initial anion state ( $a^4\Sigma_u^+, N$ ) is determined by the final rovibrational state ( $v'N'$ ) and by the rate, represented by  $\Gamma_l(R)$  [45], at which the electron is ejected in the partial wave  $l$ .

The initial and final states are both treated as Hund's case (b), since for the  $a^3\Pi_u$  state both the spin-orbit coupling constant [26] and its rotational dependence [67] are small enough that for the considered strong rotation, spin-orbit energy shifts can be neglected. The splitting of the final  $a^3\Pi_u$  states due to the  $\Lambda$ -doubling is  $< 3$  meV up to  $N' = 180$  [39, 67] and neglected in the present study.

The quartet level energies and vibrational wave functions used in averaging  $\Gamma_N(R)$  of Eq. (3) were in a first step obtained with the centroid (see Fig. 2) of the *ab initio*  $a^4\Sigma_u^+$  potential curve [45]. Calculated lifetimes for various initial  $N$ -levels are shown in Fig. 3. The lifetimes of levels within a narrow  $N$ -range spread over many orders of magnitude, as was similarly seen for the  $\text{H}_2^-$  calculations [33, 34]. Unlike these previous results, there are also well-separated groups with sets of lifetimes similar to each other on the logarithmic scale. Closer inspection reveals that the levels in such groups share the lowest angular momentum  $l$  of the ejected electron. We emphasize the following aspects of the results:

(i) Lifetimes of the experimental order of magnitude ( $\sim 10^{-3}$  s) are found for states that require  $l \geq 6$  for AD. Such states are only available for a narrow interval of initial rotational states  $N = 165$ –183. For lower  $N$ , rearrangement is not strong enough to forbid the fast AD through  $l = 2, 4$  partial waves (see Fig. 1 of the SM [45]), while higher  $N$  do not host suitable bound vibrational

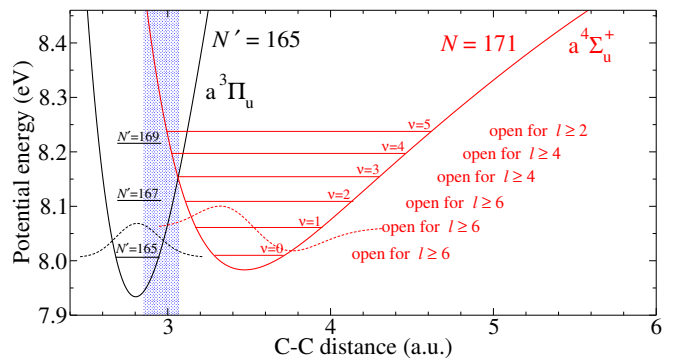


FIG. 4. Potential curves and sample vibrational wave functions (dotted) for AD with  $N = 171$  and  $N' = 165$  and relevant zone of vibrational overlap (shaded). Also shown are anionic  $v$ -levels with the  $l$ -range for which AD is energetically allowed and some  $v = 0$  neutral levels as  $N'$  increases.

levels.

(ii) The  $N'$  values required to open AD for the  $v$ -levels of given  $N$  are illustrated for  $N = 171$  in Fig. 4. The levels  $v \leq 2$  require  $N' < 167$  and hence  $l \geq 6$  from Eq. (3). In the indicated vibrational overlap zone,  $\Gamma_N$  is thus controlled by  $\Gamma_6(E)$ . Its small value reflects the threshold law  $\Gamma_l(E) \propto E^{l+1/2}$  [36], resulting in millisecond AD lifetimes for the  $N = 171, v = 0, 1, 2$  levels.

We use these calculated lifetimes  $\tau_{AD}(v, N)$  against AD for the partial wave  $l = 6$  to model the experimental neutral count rate  $s_0 = s_d + \eta s_f$  from highly excited  $\text{C}_2^-$ . The time constants  $\tau_{AD}(v, N)$  are implemented in the  $\text{C}_2^-$  unimolecular decay model of the CP [39], yielding  $s_d(t)$  for AD and  $s_f(t)$  for AF. Deriving rotational and vibrational level populations, we use bi-modal thermal distributions compatible with available evidence on sputter ion sources [39]. For the included distribution tails, this evidence suggests temperatures of  $\lesssim 1 \times 10^4$  K. When we respect this limit within the model [39], the  $a^4\Sigma_u^+$  levels turn out to be the only ones able to yield the observed AD signals. The set of  $\tau_{AD}(v, N)$  for  $l = 6$  and a parameter  $P_q$  giving the population fraction of  $a^4\Sigma_u^+$   $\text{C}_2^-$  anions with AD lifetimes of  $> 10^{-6}$  s determine the temporal trend.

The *ab initio* uncertainty of the bound  $a^4\Sigma_u^+$  potential acts on the  $\tau_{AD}(v, N)$  values. Closest agreement with the experimental signal, as shown in Fig. 1(b), is reached when this potential is increased to the upper margin of the uncertainty range, and for  $P_q = 6 \times 10^{-3}$ . When other regions within the uncertainty range are chosen, the AD decay model becomes dominated by levels with somewhat longer lifetimes [39]. The model also shows that, for the same thermal distribution, the AF signal ( $s_f$ ) stems from the tunneling dissociation of rotationally stabilized  $\text{C}_2^-$  quartet levels at high  $v$  (but at lower vibrational energy and, thus, lower vibrational temperature than would be required for  $\text{C}_2^-$  doublet levels). Correspondingly, the

modeled signals  $\eta s_f$  and  $s_d + \eta s_f$  are both shown in Fig. 1(b), where  $s_d$  mostly dominates over  $\eta s_f$ . Since AF strongly depends on vibrational excitation, other, less vibrating quartet levels with negligible AF and very long AD lifetimes in the range for  $l \geq 8$  (Fig. 3) should exist.

Using the model, we have also probed the excitation conditions of the  $C_2^-$  beam which could explain the observed AD and AF signals without a quartet  $C_2^-$  population [39]. Then, tail temperatures of  $3 \times 10^4$  K (carrying  $> 3.5\%$  of the population) are required. We consider such a scenario highly unlikely and see strong evidence for the presence of quartet levels in the investigated  $C_2^-$  ion beams.

In summary, we present a theory that predicts the AD of a diatomic molecule when it is connected with changes of rotation by as many as six quanta. The correspondingly long AD lifetimes become relevant for rotationally stabilized quartet levels of the  $C_2^-$  anion and reproduce the puzzling AD signals with long decay times observed on stored ensembles of this anion. The derived dependence of the AD width on the number of rotational quanta exchanged during the process is expected to be of general use for future treatments of strongly rotating molecular anions.

This article comprises parts of the doctoral thesis of V.C.S. submitted to the Ruprecht-Karls-Universität Heidelberg, Germany. The work of R.Č. has been supported by the Czech Science Foundation (Grant No. GACR 21-12598S). Financial support by the Max Planck Society is acknowledged. The computational results presented have been in part achieved using the HPC infrastructure LEO of the University of Innsbruck.

---

\* roman.curik@jh-inst.cas.cz

† Deceased

- [1] A. G. G. M. Tielens, The molecular universe, *Rev. Mod. Phys.* **85**, 1021 (2013).
- [2] Y. Chang, Y. Yu, H. Wang, X. Hu, Q. Li, J. Yang, S. Su, Z. He, Z. Chen, L. Che, X. Wang, W. Zhang, G. Wu, D. Xie, M. N. R. Ashfold, K. Yuan, and X. Yang, Hydroxyl super rotors from vacuum ultraviolet photodissociation of water, *Nat Commun* **10**, 1250 (2019).
- [3] Y. Chang, Y. Fu, Z. Chen, Z. Luo, Y. Zhao, Z. Li, W. Zhang, G. Wu, B. Fu, D. H. Zhang, M. N. R. Ashfold, X. Yang, and K. Yuan, Vacuum ultraviolet photodissociation of sulfur dioxide and its implications for oxygen production in the early Earth's atmosphere, *Chem. Sci.* **14**, 8255 (2023).
- [4] S. Venkataramanababu, A. Li, I. O. Antonov, J. B. Dragan, P. R. Stollenwerk, H. Guo, and B. C. Odom, Enhancing reactivity of  $SiO^+$  ions by controlled excitation to extreme rotational states, *Nat Commun* **14**, 4446 (2023).
- [5] G. S. Oehrlein and S. Hamaguchi, Foundations of low-temperature plasma enhanced materials synthesis and etching, *Plasma Sources Sci. Technol.* **27**, 023001 (2018).
- [6] A. Tappe, C. J. Lada, J. H. Black, and A. A. Muench, Discovery of superthermal hydroxyl (OH) in the HH 211 outflow, *Astrophys J* **680**, L117 (2008).
- [7] R. von Hahn, A. Becker, F. Berg, K. Blaum, C. Breitenfeldt, H. Fadil, F. Fellenberger, M. Froese, S. George, J. Göck, M. Grieser, F. Grussie, E. A. Guerin, O. Heber, P. Herwig, J. Karthein, C. Krantz, H. Kreckel, M. Lange, F. Laux, S. Lohmann, S. Menk, C. Meyer, P. M. Mishra, O. Novotný, A. P. O'Connor, D. A. Orlov, M. L. Rappaport, R. Repnow, S. Saurabh, S. Schippers, C. D. Schröter, D. Schwalm, L. Schweikhard, T. Sieber, A. Shornikov, K. Spruck, S. Sunil Kumar, J. Ullrich, X. Urbain, S. Vogel, P. Wilhelm, A. Wolf, and D. Zajfman, The cryogenic storage ring CSR, *Rev. Sci. Instrum.* **87**, 063115 (2016).
- [8] H. T. Schmidt, R. D. Thomas, M. Gatchell, S. Rosén, P. Reinhed, P. Löfgren, L. Brännholm, M. Blom, M. Björkhage, E. Bäckström, J. D. Alexander, S. Leontein, D. Hanstorp, H. Zettergren, L. Liljeby, A. Källberg, A. Simonsson, F. Hellberg, S. Mannervik, M. Larsson, W. D. Geppert, K. G. Rensfelt, H. Danared, A. Paál, M. Masuda, P. Halldén, G. Andler, M. H. Stockett, T. Chen, G. Källersjö, J. Weimer, K. Hansen, H. Hartman, and H. Cederquist, First storage of ion beams in the Double Electrostatic Ion-Ring Experiment: DESIREE, *Rev. Sci. Instrum.* **84**, 055115 (2013).
- [9] H. T. Schmidt, S. Rosén, R. D. Thomas, M. H. Stockett, W. D. Geppert, A. Larson, P. Löfgren, A. Simonsson, A. Källberg, P. Reinhed, M. Björkhage, M. Blom, J. D. Alexander, P. K. Najeeb, M. Ji, N. Kono, E. K. Anderson, G. Eklund, M. K. Kristiansson, O. M. Hole, D. Hanstorp, H. Hartman, P. S. Barklem, J. Grumer, K. Hansen, M. Gatchell, H. Cederquist, and H. Zettergren, Negative ion relaxation and reactions in a cryogenic storage ring, *J. Phys.: Conf. Ser.* **1412**, 062006 (2020).
- [10] H. M. Urbassek, Sputtering of molecules, *Nucl. Instrum. Methods Phys. Res. B* **18**, 587 (1986).
- [11] C. Anders, R. Pedrys, and H. M. Urbassek, Molecule emission from condensed Ar and  $O_2$  targets by 750 eV Ne impact, *Nucl. Instrum. Methods Phys. Res. B* **352**, 195 (2015).
- [12] C. Anders, R. Pedrys, and H. M. Urbassek, Atom and molecule emission caused by ion impact into a frozen oxygen target: Role of rovibrational excitation, *Nucl. Instrum. Methods Phys. Res. B* **315**, 308 (2013).
- [13] S. Menk, S. Das, K. Blaum, M. W. Froese, M. Lange, M. Mukherjee, R. Repnow, D. Schwalm, R. von Hahn, and A. Wolf, Vibrational autodetachment of sulfur hexafluoride anions at its long-lifetime limit, *Phys. Rev. A* **89**, 022502 (2014).
- [14] J. Fedor, K. Hansen, J. U. Andersen, and P. Hvelplund, Nonthermal power law decay of metal dimer anions, *Phys. Rev. Lett.* **94**, 113201 (2005).
- [15] E. K. Anderson, A. F. Schmidt-May, P. K. Najeeb, G. Eklund, K. C. Chartkunchand, S. Rosén, Å. Larson, K. Hansen, H. Cederquist, H. Zettergren, and H. T. Schmidt, Spontaneous electron emission from hot silver dimer anions: Breakdown of the Born–Oppenheimer approximation, *Phys. Rev. Lett.* **124**, 173001 (2020).
- [16] S. Iida, S. Kuma, H. Tanuma, T. Azuma, and H. Shimomaru, State-selective observation of radiative cooling of vibrationally excited  $C_2^-$ , *J. Phys. Chem. Lett.* **11**, 10526 (2020); Correction to "State-selective observation of radiative cooling of vibrationally excited  $C_2^-$ ",

- J. Phys. Chem. Lett.* **12**, 8980 (2021).
- [17] P. Jasik, J. Franz, D. Kedziera, T. Kilich, J. Kozicki, and J. E. Sienkiewicz, Spontaneous electron emission vs dissociation in internally hot silver dimer anions, *J. Chem. Phys.* **154**, 164301 (2021).
- [18] B. D. Rehfuß, D. Liu, B. M. Dinelli, M. Jagod, W. C. Ho, M. W. Crofton, and T. Oka, Infrared spectroscopy of carbo-ions. IV. The  $A^2\Pi_u-X^2\Sigma_g^+$  electronic transition of  $C_2^-$ , *J. Chem. Phys.* **89**, 129 (1988).
- [19] P. Yzombard, M. Hamamda, S. Gerber, M. Doser, and D. Comparat, Laser cooling of molecular anions, *Phys. Rev. Lett.* **114**, 213001 (2015).
- [20] J. U. Andersen, C. Brink, P. Hvelplund, M. O. Larsson, and H. Shen, Carbon clusters in a storage ring, *Z. Phys. D* **40**, 365 (1997).
- [21] H. B. Pedersen, C. Brink, L. H. Andersen, N. Bjerre, P. Hvelplund, D. Kella, and H. Shen, Experimental investigation of radiative lifetimes of vibrational levels at the electronic ground state of  $C_2^-$ , *J. Chem. Phys.* **109**, 5849 (1998).
- [22] M. Iizawa, S. Kuma, N. Kimura, K. Chartkunchand, S. Harayama, T. Azuma, and Y. Nakano, Photodetachment spectroscopy of highly excited  $C_2^-$  and their temporal evolution in the ion storage ring RICE, *J. Phys. Soc. Jpn.* **91**, 084302 (2022).
- [23] Preliminary results on autofragmentation and autodetachment from  $C_2^-$  presented by N. Kono, R. Paul, M. Gatchell, H. Zettergren and H. T. Schmidt at the Working-Group 1 and Working-Group 2 Conference of the COST action MD-GAS, March 15–19, 2021. (unpublished)
- [24] R. Mead, U. Hefter, P. Schulz, and W. Lineberger, Ultrahigh resolution spectroscopy of  $C_2^-$ : The  $A^2\Pi_u$  state characterized by deperturbation methods, *J. Chem. Phys.* **82**, 1723 (1985).
- [25] U. Hefter, R. D. Mead, P. A. Schulz, and W. C. Lineberger, Ultrahigh-resolution study of autodetachment in  $C_2^-$ , *Phys. Rev. A* **28**, 1429 (1983).
- [26] K. Ervin and W. Lineberger, Photoelectron spectra of  $C_2^-$  and  $C_2H^-$ , *J. Phys. Chem.* **95**, 1167 (1991).
- [27] P. Rosmus and H. Werner, Multireference-CI calculations of radiative transition probabilities in  $C_2^-$ , *J. Chem. Phys.* **80**, 5085 (1984).
- [28] J. Barsuhn, Nonempirical calculations on the electronic spectrum of the molecular ion  $C_2^-$ , *J. Phys. B: Atom. Molec. Phys.* **7**, 155 (1974).
- [29] P. W. Thulstrup and E. W. Thulstrup, A theoretical investigation of the low-lying states of the  $C_2^-$  ion, *Chem. Phys. Lett.* **26**, 144 (1974).
- [30] M. Zeitz, S. D. Peyerimhoff, and R. J. Buenker, A theoretical study of the bound electronic states of the  $C_2$  negative ion, *Chem. Phys. Lett.* **64**, 243 (1979).
- [31] W. Shi, C. Li, H. Meng, J. Wei, L. Deng, and C. Yang, Ab initio study of the low-lying electronic states of the  $C_2^-$  anion, *Comput. Theor. Chem.* **1079**, 57 (2016).
- [32] R. S. da Silva, Transition probabilities and radiative lifetimes of  $C_2^-$ : A high level theoretical investigation, *J. Quant. Spectrosc. Radiative Transfer* **321**, 109000 (2024).
- [33] R. Golser, H. Gnaser, W. Kutschera, A. Priller, P. Steier, A. Wallner, M. Čížek, J. Horáček, and W. Domcke, Experimental and theoretical evidence for long-lived molecular hydrogen anions  $H_2^-$  and  $D_2^-$ , *Phys. Rev. Lett.* **94**, 223003 (2005).
- [34] M. Čížek, J. Horáček, and W. Domcke, Long-lived anionic states of  $H_2$ , HD,  $D_2$ , and  $T_2$ , *Phys. Rev. A* **75**, 012507 (2007).
- [35] R. Marion, M. Čížek, and X. Urbain, Autodetachment spectroscopy of metastable  $D_2^-$  and  $HD^-$ , *Phys. Rev. A* **107**, 052808 (2023).
- [36] W. Domcke, Theory of resonance and threshold effects in electron-molecule collisions: The projection-operator approach, *Phys. Rep.* **208**, 97 (1991).
- [37] M. Čížek, J. Horáček, and W. Domcke, Nuclear dynamics of the  $H_2^-$  collision complex beyond the local approximation: associative detachment and dissociative attachment to rotationally and vibrationally excited molecules, *J. Phys. B: Atom. Molec. Phys.* **31**, 2571 (1998).
- [38] R. S. Berry, Ionization of molecules at low energies, *J. Chem. Phys.* **45**, 1228 (1966).
- [39] V. C. Schmidt, R. Čurík, M. Ončák, K. Blaum, S. George, J. Göck, M. Grieser, F. Grussie, R. von Hahn, C. Krantz, H. Kreckel, O. Novotný, K. Spruck, and A. Wolf, Unimolecular processes in diatomic carbon anions at high rotational excitation, Companion paper submitted to *Phys. Rev. A*.
- [40] G. Halmová, J. D. Gorfinkiel, and J. Tennyson, Low-energy electron collisions with  $C_2$  using the R-matrix method, *J. Phys. B: Atom. Molec. Phys.* **39**, 2849 (2006).
- [41] V. E. Bondybey and L. E. Brus, Photophysics of  $C_2^-$  ( $B^2\Sigma_u^+$ ) in rare gas lattices: Vibrational relaxation through intermediate  $a^4\Sigma_u^+$  levels, *J. Chem. Phys.* **63**, 2223 (1975).
- [42] W. Weltner Jr and R. J. Van Zee, Carbon molecules, ions, and clusters, *Chem. Reviews* **89**, 1713 (1989).
- [43] H. J. Werner, P. J. Knowles, R. Lindh, F. R. Knizia, F. R. Manby, M. Schütz, and Others, MOLPRO, version 2012.1, a package of ab initio programs, see <https://www.molpro.net>.
- [44] G. Halmová, *R-matrix calculations of electron-molecule collisions with  $C_2$  and  $C_2^-$* , Ph.D. thesis, University College London (2008).
- [45] See Supplemental Material containing details for the derivation of the  $F(E)$  operator for multiple electronic partial waves and for the electronic II states of the final neutral molecule, which contains Refs. [46–55].
- [46] G. Herzberg, *Molecular Spectra and Molecular Structure I. Spectra of Diatomic Molecules* (D. Van Nostrand Company, Inc., New York, 1950).
- [47] T. F. O'Malley, Theory of dissociative attachment, *Phys. Rev.* **150**, 14 (1966).
- [48] E. S. Chang and U. Fano, Theory of electron-molecule collisions by frame transformations, *Phys. Rev. A* **6**, 173 (1972).
- [49] R. J. Bieniek, Complex potential and electron spectrum in atomic collisions involving fast electronic transitions: Penning and associative ionization, *Phys. Rev. A* **18**, 392 (1978).
- [50] D. J. Haxton, C. W. McCurdy, and T. N. Rescigno, Dissociative electron attachment to the  $H_2O$  molecule I. Complex-valued potential-energy surfaces for the  $^2B_1$ ,  $^2A_1$ , and  $^2B_2$  metastable states of the water anion, *Phys. Rev. A* **75**, 012710 (2007).
- [51] M. Tarana, P. Wielgus, S. Roszak, and I. I. Fabrikant, Effects of two vibrational modes in the dissociative electron attachment to  $CF_3Cl$ , *Phys. Rev. A* **79**, 052712 (2009).
- [52] L. A. Morgan, C. J. Gillan, J. Tennyson, and X. S. Chen, R-matrix calculations for polyatomic molecules: electron

- scattering by  $\text{N}_2\text{O}$ , *J. Phys. B: Atom. Molec. Phys.* **30**, 4087 (1997).
- [53] A. U. Hazi, Behavior of the eigenphase sum near a resonance, *Phys. Rev. A* **19**, 920 (1979).
- [54] J. Macek, Behavior of eigenphases near a resonance, *Phys. Rev. A* **2**, 1101 (1970).
- [55] T. H. Dunning, Gaussian basis sets for use in correlated molecular calculations. I. The atoms boron through neon and hydrogen, *J. Chem. Phys.* **90**, 1007 (1989).
- [56] B. Jordon-Thaden, H. Kreckel, R. Golser, D. Schwalm, M. H. Berg, H. Buhr, H. Gnaser, M. Grieser, O. Heber, M. Lange, O. Novotný, S. Novotny, H. B. Pedersen, A. Petrigiani, R. Repnow, H. Rubinstein, D. Shafir, A. Wolf, and D. Zajfman, Structure and stability of the negative hydrogen molecular ion, *Phys. Rev. Lett.* **107**, 193003 (2011).
- [57] M. Čížek and K. Houfek, Nonlocal theory of resonance electron-molecule scattering, in *Low-energy electron scattering from molecules, biomolecules and surfaces*, edited by P. Čásky and R. Čurík (CRC Press, Boca Raton, 2012) 1st ed., Chap. 4, pp. 91–125.
- [58] D. J. Haxton, C. W. McCurdy, and T. N. Rescigno, Angular dependence of dissociative electron attachment to polyatomic molecules: Application to the  $^2B_1$  metastable state of the  $\text{H}_2\text{O}$  and  $\text{H}_2\text{S}$  anions, *Phys. Rev. A* **73**, 062724 (2006).
- [59] K. Houfek, M. Čížek, and J. Horáček, Calculation of rate constants for dissociative attachment of low-energy electrons to hydrogen halides HCl, HBr, and HI and their deuterated analogs, *Phys. Rev. A* **66**, 062702 (2002).
- [60] H. Hotop, M. Ruf, M. Allan, and I. I. Fabrikant, Resonance and threshold phenomena in low-energy electron collisions with molecules and clusters, *Adv. At. Mol. Opt. Phys.* **49**, 85 (2003).
- [61] M. Zawadzki, M. Čížek, K. Houfek, R. Čurík, M. Ferus, S. Civiš, J. Kočíšek, and J. Fedor, Resonances and dissociative electron attachment in HNCO, *Phys. Rev. Lett.* **121**, 143402 (2018).
- [62] T. N. Rescigno, W. A. Isaacs, A. E. Orel, H.-D. Meyer, and C. W. McCurdy, Theoretical study of resonant vibrational excitation of  $\text{CO}_2$  by electron impact, *Phys. Rev. A* **65**, 032716 (2002).
- [63] M. Čížek, J. Horáček, M. Allan, I. I. Fabrikant, and W. Domcke, Vibrational excitation of hydrogen fluoride by low-energy electrons: theory and experiment, *J. Phys. B: At. Mol. Opt. Phys.* **36**, 2837 (2003).
- [64] T. P. Ragesh Kumar, P. Nag, M. Ranković, R. Čurík, A. Knížek, S. Civiš, M. Ferus, J. Trnka, K. Houfek, M. Čížek, and J. Fedor, Electron-impact vibrational excitation of isocyanic acid HNCO, *Phys. Rev. A* **102**, 062822 (2020).
- [65] K. A. Miller, H. Bruhns, M. Čížek, J. Eliášek, R. Cabrera-Trujillo, H. Kreckel, A. P. O'Connor, X. Urbain, and D. W. Savin, Isotope effect for associative detachment:  $\text{H}(\text{D})^- + \text{H}(\text{D}) \rightarrow \text{H}_2(\text{D}_2) + e^-$ , *Phys. Rev. A* **86**, 032714 (2012).
- [66] Š. Roučka, D. Mulin, P. Jusko, M. Čížek, J. Eliášek, R. Plašil, D. Gerlich, and J. Glosík, Electron transfer and associative detachment in low-temperature collisions of  $\text{D}^-$  with H, *J. Phys. Chem. Lett.* **6**, 4762 (2015).
- [67] M. C. Curtis and P. J. Sarre, High-resolution laser spectroscopy of the Swan system ( $d^3\Pi_g-a^3\Pi_u$ ) of  $\text{C}_2$  in an organic halide-alkali metal flame, *J. Mol. Spectrosc.* **114**, 427 (1985).

## Supplementary online information

This is a supplementary material to the paper "Autodetachment of diatomic carbon anions from long-lived high-rotation quartet states" by V. C. Schmidt *et al.* This material consists of two sections. In the first section we derive the form of the complex nonlocal operator  $F(E)$  for the case of the final  $\Pi_u$  states of the neutral molecule. The second section discusses a simplified form of this operator in a local approximation. The imaginary part of the level-shift operator  $F(E)$  is expressed in terms of the partial widths  $\Gamma_l$  that are extracted from ab-initio  $R$ -matrix calculations.

### I. NONLOCAL LEVEL-SHIFT OPERATOR $F(E)$ FOR THE NEUTRAL $\Pi$ STATES

In the nonlocal resonance model, the effective Hamiltonian that drives the decaying nuclear wave function of the negative ion can be written as [1]

$$H_{\text{eff}} = T + \frac{N(N+1)}{2\mu R^2} + V_d(R) + F(E), \quad (1)$$

where the first two terms describe the rovibrational kinetic energy,  $V_d(R)$  is the discrete-state potential curve, and  $F(E)$  denotes the complex-valued level-shift operator that contains all the couplings between the resonant and continuum states of the anion in a form of a nonlocal complex-valued interaction.

The modification of the interaction operator  $F(E)$ , for our particular case, follows the ideas presented in Ref. [2]. The necessary differences arise from the intrinsic coupling of the degenerated electronic non- $\Sigma$  states with the molecular rotations [3]. Therefore, the neutral target electronic state  $w(\tau)$  will also enter the derivation. The symbol  $\tau$  here represents, collectively, the space coordinates of the target electrons. Note that the anion state is still considered to be in the  $\Lambda = 0$  state, presently the  $C^4\Sigma_u^+$  state of  $C_2^-$ . We start from the definition of the  $F(E)$  by T.F. O'Malley [4]

$$F(E) = \langle d|QHPPG_pPHQ|d\rangle, \quad (2)$$

where  $Q$  and  $P$  are the projection operators [4, 5],  $G_p = 1/P(E - H + i\epsilon)P$ , the discrete state of the anion is represented by  $|d\rangle$ , and the total Hamiltonian can be written as a sum of the nuclear kinetic energy  $T$  and of the electronic Hamiltonian  $H_{\text{el}}$ , i.e.  $H = T + H_{\text{el}}$ . The projection operator  $P$  can be expressed in the adiabatic energy-normalized eigenstates  $|\mathbf{k}^{(+)}\rangle$  of the  $PH_{\text{el}}P$  operator as [2]

$$P = \int d\mathbf{k} |\mathbf{k}^{(+)}\rangle \langle \mathbf{k}^{(+)}|. \quad (3)$$

After inserting the expansion (3) into Eq. (2) we can write

$$F(E) = \int d\mathbf{k} d\mathbf{q} \langle d|H_{\text{el}}|\mathbf{k}^{(+)}\rangle \langle \mathbf{k}^{(+)}|G_p|\mathbf{q}^{(+)}\rangle \langle \mathbf{q}^{(+)}|H_{\text{el}}|d\rangle. \quad (4)$$

The anion's background states  $|\mathbf{k}^{(+)}\rangle$  are first written in the body frame coordinates  $\mathbf{r}'$  and  $\tau$

$$\langle \mathbf{r}'|\mathbf{k}^{(+)}\rangle = \frac{1}{\sqrt{2}} \mathcal{A} \sum_{l'} \frac{1}{r'} \left[ w_{\Lambda}(\tau) \phi_{ll'}^{-\Lambda}(k, r') Y_{l-\Lambda}(\hat{\mathbf{r}}') Y_{l'-\Lambda}^*(\hat{\mathbf{k}}') + \eta w_{-\Lambda}(\tau) \phi_{ll'}^{\Lambda}(k, r') Y_{l\Lambda}(\hat{\mathbf{r}}') Y_{l'\Lambda}^*(\hat{\mathbf{k}}') \right], \quad (5)$$



where the symbol  $\mathcal{A}$  antisymmetrizes the wave function with respect to the exchange of the anion's electronic coordinates. Quantum number  $\eta$  denotes the parity of the anion state with respect to the reflection on the body-frame coordinate plane ( $x'z'$ ), that changes  $w_\Lambda$  into  $(-1)^\Lambda w_{-\Lambda}$  [6]. Recall that  $w_\Lambda$  and  $w_{-\Lambda}$  are different but degenerate for  $\Lambda \neq 0$ . For simplicity, the anionic wave function in the above equation is already assumed to possess the  $\Sigma_u^+$  symmetry as the neutral target state  $w_\Lambda$  couples only with the continuum wave function with the  $-\Lambda$  projection of its angular momentum  $l$  onto the molecular axis.

The matrix elements

$$V_{d\mathbf{k}} = \langle d|H_{\text{el}}|\mathbf{k}'^{(+)}\rangle \quad (6)$$

in Eq. (4) are first written in the body frame of reference as

$$V_{d\mathbf{k}'} = \frac{1}{\sqrt{2}} \sum_{l'} \left[ V_{dkl'}^{-\Lambda} Y_{l'-\Lambda}^*(\hat{\mathbf{k}}') + \eta V_{dkl'}^{\Lambda} Y_{l'\Lambda}^*(\hat{\mathbf{k}}') \right], \quad (7)$$

with

$$V_{dkl'}^{\Lambda} = \sum_l \langle d|H_{\text{el}}|\mathcal{A} \frac{1}{r} w_{-\Lambda} \phi_{l'}^{\Lambda} Y_{l\Lambda}\rangle. \quad (8)$$

Note that  $V_{dkl'}^{\Lambda} = V_{dkl'}^{-\Lambda}$  because both terms on the r.h.s. of Eq. (5) must be of  $\Sigma_u^+$  symmetry and the azimuthal parts of the target and continuum wave functions must cancel [3].

There is one more simplification introduced in Eq. (5) and it is omission of a sum over the target states  $w(\tau)$  accounting for the correlation and polarization effects between the ejected electron and the neutral molecule. Such a sum would slightly change the definition of  $V_{dkl'}^{\Lambda}$  since the sum would appear in the ket on the r.h.s of Eq. (8). Moreover, this sum would also enable the theory for the autodetachment decay into multiple final electronic states. However, these excited  ${}^3\Pi_u$  states do not contribute into the present study and thus they are omitted for clarity.

The  $V_{d\mathbf{k}'}$  term in (6) and (7) is a component of the level-shift operator  $F(E)$  in Eq. (4) and it depends on the momentum vector  $\mathbf{k}'$  expressed in the body frame of reference. Transformation to the unprimed coordinates attached to the laboratory frame is easily done through the Wigner D-functions as

$$V_{d\mathbf{k}} = \frac{1}{\sqrt{2}} \sum_{l'm} \left[ V_{dkl'}^{\Lambda} D'_{-\Lambda m}(\hat{\mathbf{R}}) + \eta V_{dkl'}^{-\Lambda} D'_{\Lambda m}(\hat{\mathbf{R}}) \right] Y_{l'm}^*(\hat{\mathbf{k}}), \quad (9)$$

where the unit vector  $\hat{\mathbf{R}}$  stands for the Euler angles of the diatomic molecule's orientation in the laboratory frame, i.e.  $\hat{\mathbf{R}} \equiv (0, \theta, \phi)$ .

The second term in the integral on the r.h.s of Eq. (4) represents the nuclear propagator

$$\langle \mathbf{k}^{(+)}|G_p|\mathbf{q}^{(+)}\rangle = \langle \mathbf{k}^{(+)}|(E - q^2/2 - T - V_0(R) + i\epsilon)^{-1}|\mathbf{q}^{(+)}\rangle = \langle \mathbf{k}^{(+)}|G_0(E - q^2/2)|\mathbf{q}^{(+)}\rangle, \quad (10)$$

where  $V_0(R)$  is the adiabatic potential energy curve of the neutral molecule in degenerate states  $w_\Lambda$ ,  $w_{-\Lambda}$ , and  $G_0$  is the Green's function of the neutral molecule [2, 7]. This Green's function can be expanded in the rovibrational eigenfunctions

$$Z_{\nu'N'M'}^{\Lambda\eta'}(\tau, \mathbf{R}) = \frac{1}{R} \chi_{\nu'N'}(R) X_{N'M'}^{\Lambda\eta'}(\tau, \hat{\mathbf{R}}), \quad (11)$$

where the rotational wave function of the neutral molecule, in the non- $\Sigma$  electronic state, can be written as follows [6]:

$$X_{N'M'}^{\Lambda\eta'}(\tau, \hat{\mathbf{R}}) = \left( \frac{2N'+1}{8\pi} \right)^{1/2} \left[ w_\Lambda(\tau) D_{\Lambda M'}^{N'}(\hat{\mathbf{R}}) + \eta' w_{-\Lambda}(\tau) D_{-\Lambda M'}^{N'}(\hat{\mathbf{R}}) \right]. \quad (12)$$

Similar to anion case in Eq. (5) the symbol  $\eta'$  represent the  $(x'z')$ -plane-reflection parity for the final neutral molecule. The expansion into the rotational states

$$G_0^{\Lambda\eta'}(E, \mathbf{R}, \mathbf{R}') = \sum_{N'M'} X_{N'M'}^{\Lambda\eta'}(\hat{\mathbf{R}}) \frac{1}{R} G_{0N'}(E, R, R') \frac{1}{R'} X_{N'M'}^{*\Lambda\eta'}(\hat{\mathbf{R}}'), \quad (13)$$

is then followed by the expansion of the radial Green's function into the vibrational states

$$G_{0N'}(E, R, R') = \sum_{\nu'} \frac{\chi_{\nu'}(R)\chi_{\nu'}(R')}{E - E_{\nu'N'} + i\epsilon}. \quad (14)$$

The energy levels  $E_{\nu'N'}$  are rovibrational energies of the neutral system.

All the ingredients are now prepared to evaluate the angular matrix elements of the level-shift operator  $F(E)$  defined by Eq. (4), i.e.

$$\langle Y_{N_1M_1} | F(E) | Y_{N_2M_2} \rangle = \frac{1}{RR'} \delta_{N_1N_2} \delta_{M_1M_2} f_{N_1}(E, R, R'), \quad (15)$$

where the radial component of the level-shift operator is defined as

$$f_N(E, R, R') = \sum_{lN'} \frac{1}{2} \left[ 1 + \eta'(-1)^{l+N'+N} \right] (2N' + 1) \begin{pmatrix} l & N' & N \\ \Lambda & -\Lambda & 0 \end{pmatrix}^2 \times \int dk k V_{dkl}^{\Lambda}(R) G_{0N'}(E - k^2/2, R, R') V_{dkl}^{*\Lambda}(R'). \quad (16)$$

The remaining steps just follow Refs. [2, 5]. The integration over the momentum in Eq. (16) can be done analytically because of the resolvent form (14) of  $G_{0N'}$ . The level-shift operator is by this integration split into the real and imaginary components:

$$f_N(E, R, R') = \sum_{lN'} \frac{1}{2} \left[ 1 + \eta'(-1)^{l+N'+N} \right] (2N' + 1) \begin{pmatrix} l & N' & N \\ \Lambda & -\Lambda & 0 \end{pmatrix}^2 \times \sum_{\nu'} \chi_{\nu'N'}(R) \left[ \Delta_l(E - E_{\nu'N'}, R, R') - \frac{i}{2} \Gamma_l(E - E_{\nu'N'}, R, R') \right] \chi_{\nu'N'}(R'), \quad (17)$$

where

$$\Gamma_l(\varepsilon, R, R') = 2\pi V_{dkl}^{\Lambda}(R) V_{dkl}^{*\Lambda}(R'), \quad (18)$$

$$\Delta_l(\varepsilon, R, R') = \frac{1}{2\pi} \mathcal{P} \int d\varepsilon' \frac{\Gamma_l(\varepsilon', R, R')}{\varepsilon - \varepsilon'}. \quad (19)$$

While the expressions (16) and (17) are very similar to the ones derived in Ref. [2], the factor  $g_{lN'N}^{\eta'} = (1 + \eta'(-1)^{l+N'+N})/2$  is new for the case  $\Lambda \neq 0$ . In order to understand this two-valued factor (0 or 1), we first note that due to the bosonic nuclear spin statistics of the present  $C_2^-$  system, only the odd rotational quanta  $N$  of the decaying anion are populated. Furthermore, in the studied process the  $\Sigma_u$  anion decays into the  $\Pi_u$  neutral molecule and hence the continuum electron must be of the  $\Pi_g$  symmetry, which contains only the even quanta of the ejected electron's angular momenta  $l$ . Finally, each of the final neutral rotational levels  $N'$  is nearly doubly degenerate, split by the  $\Lambda$ -doubling effect. One of the states in this pair is symmetric and the other is antisymmetric with respect to the nuclear exchange. The upper and the lower components are distinguished by the sign of  $\eta'$  [3]. Therefore the factor  $g$  simply selects only those final rotational states of

the neutral molecule, that are compatible with the nuclear spin conservation during the AD decay process.

The spherical symmetry of the level-shift operator  $F(E)$  demonstrated by Eq. (15) suggests that, in the present model, different initial rotational levels  $N$  are not coupled. However, every one of these initial levels can decay into those final states (each represented by the rotational quantum  $N'$  of the neutral molecule and ejected electron's angular momentum  $l$ ) that are allowed in the sum on the r.h.s. of Eq. (17). Furthermore, it is clear that the AD decay lifetimes into the final states are controlled by the partial widths  $\Gamma_l$ .

## II. LOCAL APPROXIMATION AND THE PARTIAL WIDTHS $\Gamma_l$

The localization of the nonlocal operator  $F(E, R, R')$  is a commonly used technique [2, 5, 7, 8] exploiting different timescales of the electronic and nuclear motions. The interaction and the centrifugal terms of the radial Schrödinger equation are written as

$$\frac{N(N+1)}{2\mu R^2} + V_d(R) + f_N(R) = \frac{N(N+1)}{2\mu R^2} + V_N^{\text{loc}}(R) - \frac{i}{2}\Gamma_N^{\text{loc}}(R), \quad (20)$$

where

$$V_N^{\text{loc}}(R) = V_0(R) + E_N^{\text{res}}(R) = V_d(R) + \Delta_N(E_N^{\text{res}}(R), R, R), \quad (21)$$

$$\Gamma_N^{\text{loc}}(R) = \Gamma_N(E_N^{\text{res}}(R), R, R). \quad (22)$$

In the present study we neglect the  $N$ -dependence of the resonance energy  $E^{\text{res}}$  as the resonance is dominantly localized in a single partial wave  $l = 2$ . In this case the term  $\Delta_l$  can be taken out of the sums in Eq. (17) and what remains, in the real part of  $f_N$ , is the resolution of identity. We estimate the error in the  $V^{\text{loc}}$  caused by this assumption in order of a few meV in the present study. Such a simplification will not be done for the imaginary part of the radial level-shift operator, because we want to explore the decay lifetimes over many orders of magnitude. Therefore, the  $\Gamma_N^{\text{loc}}$  remains as

$$\Gamma_N^{\text{loc}}(R) = \sum_{lN'\nu'} g_{lN'N}^{\nu'} (2N'+1) \begin{pmatrix} l & N' & N \\ \Lambda & -\Lambda & 0 \end{pmatrix}^2 \Gamma_l^{\text{loc}}(R) |\chi_{\nu'N'}(R)|^2. \quad (23)$$

Because the crossing point between the anion's and neutral curve depends on both rotational quantum numbers  $N$  and  $N'$ , it would be very difficult to construct the  $R$ -dependent width function  $\Gamma_l^{\text{loc}}(R)$ . Instead, we opt to replace the  $R$ -parameterized version of the local approximation by the energy parameterization, i.e.

$$\Gamma_l^{\text{loc}}(E^{\text{res}}) = \Gamma_l(E^{\text{res}}, R(E^{\text{res}}), R(E^{\text{res}})). \quad (24)$$

Such parameterization has been previous used to characterize the two-dimensional resonant surface of the  $\text{CF}_3\text{Cl}$  molecule [9].

The partial widths were obtained at the neutral equilibrium geometry by calculations of the energy-dependent  $K$  matrices with the diatomic UK R-matrix package [10]. An example of the eigenphases, one of the ingredients to determine the partial widths, is shown in the left panel of Fig. 1. The figure demonstrates that the resonant state is strongly localized in a single eigenphase channel that should not be mistaken for the angular momentum channel. This single eigenphase channel still consists of several partial waves with a dominant  $d$ -wave contribution. The technique for extraction of the partial widths was adopted from [11, 12]. The background  $S$  matrix  $S^0$  first diagonalized

$$\underline{U}^+ \underline{S}^0 \underline{U} = e^{2i\delta^0}, \quad (25)$$

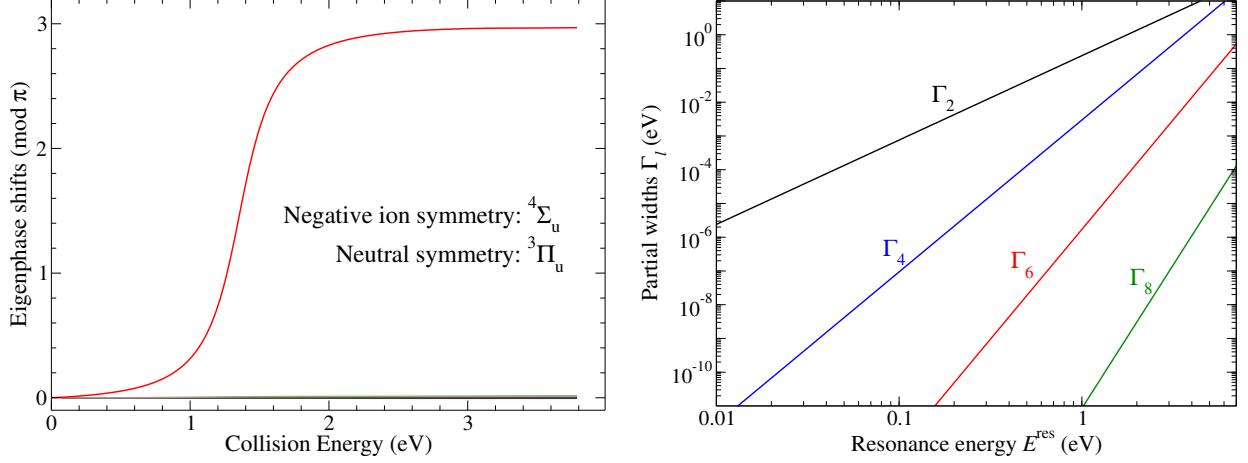


FIG. 1. Left panel: Eigenphases in the  $4\Sigma_u$  symmetry as functions of the collision energy. The nuclei are fixed at the equilibrium distance  $R_0 = 2.49$  bohrs. Right panel: The energy dependence of the partial widths  $\Gamma_l^{\text{loc}}(E^{\text{res}})$ .

where  $\underline{\delta}^0$  is the diagonal matrix of the background eigenphases  $\delta_\alpha^0$ . According to Macek [13], the partial widths can be obtained by fitting the energy dependence of the eigenphases

$$2(E - E^{\text{res}}) = \sum_{\alpha} \Gamma_{\alpha} \cot [\delta_{\alpha}^0 - \delta_{\beta}(E)] \quad (26)$$

for every eigenphase  $\delta_{\beta}(E)$ . The symbol  $E^{\text{res}}$  denotes the resonance energy and  $\Gamma_{\alpha}$  describe partial widths of the decay into the eigenchannels of the background  $S$  matrix  $S^0$ . However, our LCP model requires partial widths  $\Gamma_l$  describing decays into the different partial waves of the continuum electron.

The partial widths  $\Gamma_l$  can be obtained once the full  $S$  matrix is transformed into the background eigenchannels as

$$\underline{U} \underline{A} \underline{U}^+ = \underline{S}. \quad (27)$$

While the matrix  $\underline{A}$  is diagonal for  $\underline{S}^0$ , it contains rank-1 additional resonant term for the full matrix  $\underline{S}$  [13]:

$$A_{\alpha\beta} = e^{i\delta_{\alpha}^0} \left[ \delta_{\alpha\beta} - i \frac{(\Gamma_{\alpha}\Gamma_{\beta})^{1/2}}{E - E^{\text{res}} + i\Gamma/2} \right] e^{i\delta_{\beta}^0}. \quad (28)$$

This leads directly to

$$\Gamma_l^{1/2} = \sum_{\alpha} U_{l\alpha} \Gamma_{\alpha}^{1/2}, \quad (29)$$

where  $U_{l\alpha}$  are the eigenvectors of the background  $S$  matrix  $S^0$  in Eq. (27) and the eigenchannel partial widths  $\Gamma_{\alpha}$  are obtained by fitting the formula (26).

The partial widths from the equilibrium geometry, and from the corresponding resonant energy  $E^{\text{res}}(R_{\text{eq}})$ , were then extrapolated to other geometries by an application of the threshold law  $\Gamma_l(\varepsilon) \sim \varepsilon^{l+1/2}$  [5]. The resulting energy dependence of the partial widths is shown in the right panel of Fig. 1.

While the resonant part of the anion curve was described in the previous section, the neutral and anion bound-state curves were obtained by the internally contracted Multi-Reference Configuration Interaction (MRCI) as implemented in MOLPRO 12 package of quantum-chemistry programs [14]. The wavefunctions for the MRCI method were generated by the state-averaged Multi-Configuration Self-Consistent Field (MCSCF) method with the active space of 8 and 9 electrons in 8 orbitals for  $C_2$  and  $C_2^-$ , respectively. Molecular orbitals were described by the Dunning's augmented correlation-consistent basis of quadruple-zeta quality aug-cc-pVQZ [15]. The energies of the  $A^3\Pi_u$  neutral and

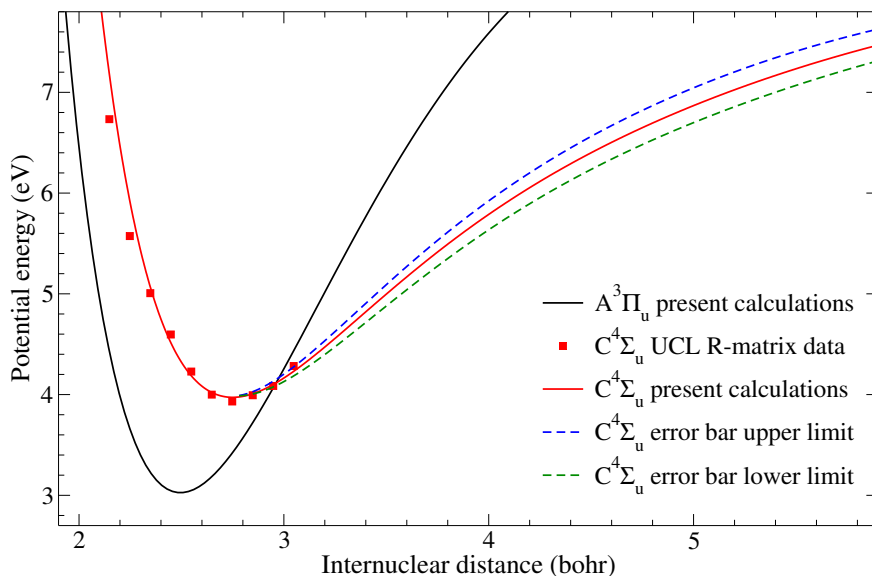


FIG. 2. Potential curves for the relevant neutral and anion states. The present calculations are shown with the full curves. Previous  $R$ -matrix calculations [16, 17] are displayed with squares. The dashed lines represent our estimate of the error bars for the present anion curve calculations.

$C^4\Sigma_u^+$  anion states, resulted from the present calculations, are displayed as the full curves in Fig. 2. These data together with the energy-dependent partial widths, shown in the right panel of Fig. 1, constitute all the electronic structure information necessary to build the effective Hamiltonian  $H_{\text{eff}}$  in Eq. (1) in the local complex approximation.

It is worth to note, that the present quartet anion curve was already studied previously by Halmová *et al.* [16, 17]. While the partial widths  $\Gamma_l$  were not analyzed in Refs. [16, 17], the resonance energy  $E^{\text{res}}$  agrees reasonably well with the present calculations (see Fig. 2). However, the major discrepancy lies in the total resonance width  $\Gamma$ . Halmová [17] reports  $\Gamma(R_{\text{eq}}) = 0.28$  eV, while in the present calculations  $\Gamma(R_{\text{eq}}) = 0.48$  eV.

Finally, in order to estimate an impact of the accuracy of our *ab initio* calculations on the final results, we introduce computational error bars in form of upper- and lower-limit anion curves as shown in Fig. 2 by the dashed lines. These curves reach maximum deviations  $\pm 170$  meV from the unperturbed  $C^4\Sigma_u$  curve at  $R = 5$  bohrs. The value of the deviation is chosen arbitrarily, as our estimate for the typical error in the correlation energy for  $\pi$ -bonded systems described by the MRCI method.

---

[1] M. Čížek, J. Horáček, and W. Domcke, Phys. Rev. A **75**, 012507 (2007).

- [2] M. Čížek and K. Houfek, in *Low-energy electron scattering from molecules, biomolecules and surfaces*, edited by P. Čárský and R. Čurík (CRC Press, Boca Raton, 2012) 1st ed., Chap. 4, pp. 91–125.
- [3] G. Herzberg, *Molecular Spectra and Molecular Structure I. Spectra of Diatomic Molecules* (D. Van Nostrand Company, Inc., New York, 1950).
- [4] T. F. O'Malley, Phys. Rev. **150**, 14 (1966).
- [5] W. Domcke, Phys. Rep. **208**, 97 (1991).
- [6] E. S. Chang and U. Fano, Phys. Rev. A **6**, 173 (1972).
- [7] R. J. Bieniek, Phys. Rev. A **18**, 392 (1978).
- [8] D. J. Haxton, C. W. McCurdy, and T. N. Rescigno, Phys. Rev. A **75**, 012710 (2007).
- [9] M. Tarana, P. Wielgus, S. Roszak, and I. I. Fabrikant, Phys. Rev. A **79**, 052712 (2009).
- [10] L. A. Morgan, C. J. Gillan, J. Tennyson, and X. S. Chen, J. Phys. B: Atom. Molec. Phys. **30**, 4087 (1997).
- [11] A. U. Hazi, Phys. Rev. A **19**, 920 (1979).
- [12] D. J. Haxton, C. W. McCurdy, and T. N. Rescigno, Phys. Rev. A **73**, 062724 (2006).
- [13] J. Macek, Phys. Rev. A **2**, 1101 (1970).
- [14] H. J. Werner, P. J. Knowles, R. Lindh, F. R. Knizia, F. R. Manby, M. Schütz, and Others, MOLPRO, version 2012.1, a package of ab initio programs (2012).
- [15] T. H. Dunning, J. Chem. Phys. **90**, 1007 (1989).
- [16] G. Halmová, J. D. Gorfinkiel, and J. Tennyson, J. Phys. B: Atom. Molec. Phys. **39**, 2849 (2006).
- [17] G. Halmová, *R-matrix calculations of electron-molecule collisions with  $C_2$  and  $C_2^-$* , Ph.D. thesis, University College London (2008).